

Thermodynamic Stable Site for Interstitial alloy (N or O) in bcc-Refractory Metals using Density Functional Theory

Henry Martin^{a,b}, Peter Amoako-Yirekyi^{a,c,*}, Eric K. K. Abavare^b

^a*Center for Scientific and Technical Computing, National Institute for Mathematical Sciences, Kumasi, Ghana*

^b*Department of Physics, Kwame Nkrumah University of Science and Technology, Kumasi, Ghana*

^c*Department of Mathematics, Kwame Nkrumah University of Science and Technology, Kumasi, Ghana*

Abstract

Plasticity in body centered cubic (bcc) refractory metals are largely due to the stress tensor induced either by solute or thermal activation. The mechanism of the solute atom(s) residence causes instability in such metals. Earlier research have considered the mechanism of oxygen (O) or carbon (C) in tungsten (W), even though the major component of the environment is nitrogen (N). In this article, the density functional theory (DFT) was employed to investigate the thermodynamic stable site for an interstitial solute (N or O) in the bcc refractory metals (Mo and Nb) by calculating the equilibrium and structural parameters, dissolution energetics and volumetric strain. The dissolution mechanism of all the relaxed solid solution structures were predicted to be an exothermic reaction from the supersaturated cell to the low concentration (1.82 at.%) except for Mo-N solid solution. Convergence of volumetric strain was observed at the low concentration of the solute. At this point, the solid solution of Mo-N and Mo-O had a less measure of global stress (less distortion) at the octahedral (o) site while that of Nb-N and Nb-O were at the tetrahedral (t) site. This certainly shows why this two bcc-refractory metals in groups VB (Nb) and VIB

*Peter Amoako-Yirekyi

Email address: hmartin@knust.edu.gh/amoakoyirekyi@knust.edu.gh (Peter Amoako-Yirekyi)

(Mo) of the periodic table exhibit different deformation behaviours giving their difference in site preference stability.

Keywords: **Stable site**, Thermodynamics, Solid solution, bcc-refractory-interstitial, DFT

1. Introduction

Body centered cubic (bcc) refractory metals have extraordinary resistance to wear and heat giving their unusual high melting point [1]. They also have high hardness value at room temperature and are chemically inert with relatively high density [2]. These metals are relatively abundant naturally in the earth's crust as mineral compounds of oxides and sulfides, Figure 1 depicts few of such elements [3]. The Niobium mineral: *Pyrochlore* $((Ca, Na)_{2-m}Nb_2O_6(O, OH, F)_{1-n}xH_2O)$ and *Columbite* $((Fe, Mn)(Nb, Ta)_2O_6)$ are forms for obtaining its ore deposits. The only sulfide compound mineral is *Molybdenite* (MoS_2) , which is found as veins in quartz rock [3].

Nb 2.4×10^{-3}	Mo 2.3×10^{-4}	<div style="display: flex; align-items: center; gap: 10px;"> <div style="border: 1px solid blue; width: 20px; height: 10px; display: inline-block;"></div> Oxides, complex oxides <div style="border: 1px solid red; width: 20px; height: 10px; display: inline-block; margin-left: 20px;"></div> Sulfides </div>
Ta 2.1×10^{-4}	W 1.0×10^{-4}	

Figure 1: Natural forms of some refractory metals with relative percentage abundance aligned in groups VB and VIB of the periodic table [3]

According to the Kepler conjecture, bcc crystal structures are less dense in comparison with fcc (ccp) and hcp [4, 5]. This, at low temperature warrants different behaviours in these structures during plastic deformation [6, 7, 8]. Particularly at decreasing temperature, there exist rapid increase in the flow stress and strain rate of single crystals (thus, bcc metals) [9, 10, 11, 12] which is mainly caused by breakdown in the standard geometric projection (non-glide components added to the stress tensor) [13, 14] during plastic deformation by solute

[15, 16] or thermal activation [17, 18, 19].

Many researchers have established that the bcc refractory metals of groups VB (V, Nb, and Ta) and VIB (Cr, Mo, and W) exhibit different deformation behaviours [20, 21, 22]. This difference is ascribed to the different behaviours of domination of screw dislocation motion at the cores during plastic deformation at low temperatures [20, 23, 24]. Woodward and Rao demonstrated that the periodic table elements of group VB (Nb) has screw displacement spreading evenly about a central point while group VIB (Mo) are off centred [25, 26, 27, 28].

At lower temperatures, these bcc refractory metals display poor fracture toughness. Hence, the need to consider alloying with other elements to improve their ductility. A known technique called solid solution for producing novel materials has played significant role from the Bronze Age through the Iron Age to these advanced technological times [29, 30]. This technique has so far caused a significant change in the application of bcc metals strengthening (softening or hardening). [31, 32, 33]. From the onset of this solid solution technique, several researches (experimentally and computationally) have sought to investigate and understand substitutional solid solution [16, 34, 17, 35, 18, 19, 36, 37, 38, 39, 40]. Unfortunately, little attention has been given to the interstitial solid solution [41, 42, 43].

However, some research has demonstrated that interstitial solutes such as B, C, N, O in bcc transition metal (Fe) stabilizes the hard core configuration of screw dislocation [38, 28, 44, 45]. Recently, similar research has been done in bcc-refractory metal for C in (V, Nb, Ta, Mo and W) and O in W [41, 43]. These interstitial solutes have also been proven to produce a marked increase in the ductile-to-brittle transition temperature (DBTT) of bcc metals. This relation to DBTT effect is linked to the dislocation motion at a specific temperature level. A reduction of the kinetic energy (cause of low temperature) of the atoms slows the movement of dislocation in order for plasticity to take place. Typically, the addition of O and N to high pure crystals of Nb and Ta causes hardening [46, 47]. However, research show that the hardness of Nb decrease with increasing Nb concentration [48, 49, 50, 51]. This shows the presence of

the interstitial solutes retards the dislocation motion for the occurrence of plasticity.

Given the importance of these bcc refractory interstitial solid solution in various applications where their plastic response ranges across length, time, and temperature scales. It is critical that we understand their performance and stability in any applicable regime on any scale [52, 53].

This paper addresses the thermodynamic mechanism occupancy preference of the interstitial solutes in bcc refractory metals. This was accomplished by using DFT because of the experimental difficulty of studying and measuring the effects of atomic distributions and external stresses on thermodynamic properties [54]. The use of DFT offers an opportunity such as accessing the compositional temperature range of interest. This grants the ability to describe the deformation as well as to provide the essential chemical details of the interaction. Characteristics such as the equilibrium geometries, dissolution energetics and volumetric strain of the systems (MoN, NbN, NbO and MoO) were the center of focus for our investigation and analysis.

2. Computational Method

The Density Functional Theory (DFT) formulation [55, 56] as implemented in the Vienna ab initio Simulation Package (VASP) [57, 58, 59] was employed. In employing DFT in the VASP package a construction of different sizes of supercell using a range of $1 \times 1 \times 1$ to $3 \times 3 \times 3$ was first done to depict different concentration of solute in the bcc refractory metal. This was done such that one interstitial solute (N or O) is inserted within an octahedral or tetrahedral sites of the bulk system (supercell of Mo or Nb) as shown in Figure 2.

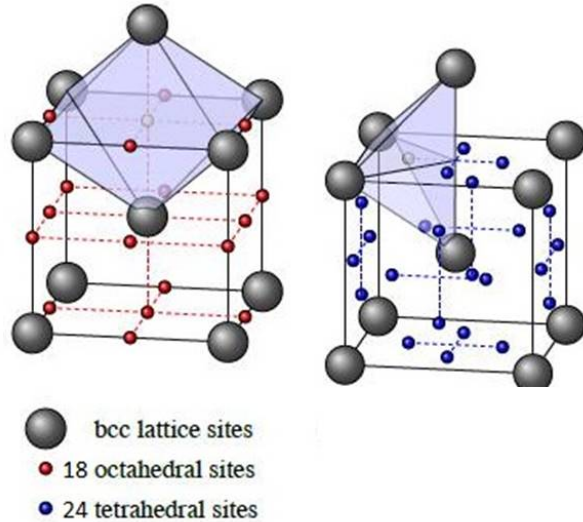


Figure 2: Octahedral and tetrahedral sites of bcc unit cell [43]

The Projector Augmented Wave (PAW) pseudopotential scheme [60, 61] with semi-core p states was considered as part of the valence electrons for the bcc refractory metals [62, 63, 64]. The Perdew-Burke-Ernzerhof (PBE) functional [65, 66] within the Generalized Gradient Approximation (GGA) [67], together with the Hermite-Gaussian within the Methfessel and Paxton method [68, 69, 70] were employed with an appropriate smearing sigma to obtain a negligible energy difference value less than 1 meV/atom.

The convergence of kinetic energy cut-off was found with appropriate k-points leading to a stable thermodynamic system. For an accurate and validated comparison, the kinetic energy cut-off and the k-point chosen for a particular supercell structure (example Mo) is used for all systems except that of the molecules ($A_2 = N_2$ or O_2). The systems used k-point sampling of $7 \times 7 \times 7$, $3 \times 3 \times 3$ and $3 \times 3 \times 3$ for X_2 , X_{16} and X_{54} respectively. Where, X represent all systems. The molecules were computed by placing the dimer in a cubic box after which a Γ point calculation was carried out. The modified Broyden's method was applied for the final step of charge mixing scheme [71]. The relaxation of both cell shape and atomic positions structures were performed until forces on each atom was

less than 10^{-5} eV/atom using the Conjugate Gradient (CG) technique.

The total energies of the interstitial solutes and the bulk refractory metals were obtained to calculate the dissolution energy or the heat of solution at a specific x-site ($x = \{o \text{ or } t\}$), E_{d_x} as

$$E_{d_x} = E_{\text{bcc cell+IS}} - E_{\text{bcc cell}} - \frac{1}{2}E[\text{A}_2] \quad (1)$$

Where $E_{\text{bcc cell+IS}}$ and $E_{\text{bcc cell}}$ are the energies for bulk bcc refractory metal with and without an inserted interstitial solute respectively. The last term defines the energy of the molecular atom being considered. The dissolution energy difference, $\Delta E_{d_{o-t}}$, with respect to the difference in the occupied site ($x = \{o \text{ or } t\}$) was also obtained. Finally, the volume of the supercells were obtained after the relaxation of the whole system with and without the interstitial solute. This was done to calculate the volumetric strain which is equivalent to hydrostatic strain as follows:

$$\epsilon_v = \frac{\Delta V}{V} \approx \text{Tr}(\epsilon) = 3\epsilon \quad (2)$$

3. Results and Discussion

In determining the thermodynamic stable site of bcc refractory interstitial solid solution using the DFT technique, the equilibrium geometries were first obtained. The lattice constant of the bulk bcc refractory metals (Mo and Nb) and the vibration frequency of the dimers (N_2 and O_2) are shown in Table 1. These as shown in the same Tables are within the range of experimental data as well as previously calculated DFT results.

Table 1: PAW-DFT-GGA predictions of lattice parameters (a) of bcc refractory metals (Mo and Nb) and the vibration frequency (cm^{-1}) of the dimers (N_2 and O_2 gas) together with some other computational and experimental results are also shown for comparison

Specie	a (\AA)	Specie	a (\AA)	Dimers	Freq (cm^{-1})
Mo	3.0996 ^a	Nb	3.294 ^g		2359 ^m
	3.142 \pm 0.03 ^b		3.296 ^h	N_2 (<i>gas</i>)	2566.28 ⁿ
	3.15 ^{c,d}		3.300 ^{i,j}		2579.48^q
	3.16 ^e		3.312 ^k		1556 ^o
	3.17 ^f		3.326 ^l	O_2 (<i>gas</i>)	1645.1^q
	3.17^q		3.327^q		2359 ^p

^a Ref.[16] ^b Ref.[72] ^c Ref.[73] ^d Ref.[74] ^e Ref.[75] ^f Ref.[63] ^g Ref.[73]

^h Ref.[76] ⁱ Ref.[77] ^j Ref.[78] ^k Ref.[79] ^l Ref.[80] ^m Ref.[81] ⁿ Ref.[82]

^o Ref.[83] ^p Ref.[84] ^q This work

As displayed in Figure 2, the experimental lattice parameter (a) and atomic radius (r) of the bcc refractory metals (Mo is 3.15 \AA and 1.363 \AA and Nb is 3.30 \AA and 1.430 \AA respectively) were replaced in a theoretical formulae given as:

$$\frac{r_o}{r} = \frac{a(\frac{1}{2} - \frac{\sqrt{3}}{4})}{a\frac{\sqrt{3}}{4}} \quad (\text{o-site})$$

$$\frac{r_t}{r} = \frac{a(\frac{\sqrt{5}}{4} - \frac{\sqrt{3}}{4})}{a\frac{\sqrt{3}}{4}} \quad (\text{t-site})$$

to obtain the radii of the o-site (r_o) and t-site (r_t) for Mo as 0.21086 \AA and 0.39663 \AA , respectively and for Nb as 0.22122 \AA and 0.41612 \AA , respectively. N and O has a covalent radius of 0.74 \AA and 0.66 \AA respectively. Therefore, the expectation would be that N and O will fit better in the t-site with less distortion, given that the radius at the t-site is wider than that of the o-site for fixed atoms position or Unrelaxed structure. We note that this theoretical expectation do not account for any form of relaxation within the geometry of the bcc lattice.

In confirming this assertion from the theoretical formulae, we first assess Table 2

- 5 showing the dissolution energy difference of N and O occupancy in the o-site and t-site of bcc refractory metals supercell sizes using different concentration of N and O. Since the difference in dissolution energy determines the minimum energy at a particular site, the stability is gained for the alloying element located in the pure metal (bcc-refractory interstitial solid solution). It can be expressed as:

$$\Delta E_{d_{o-t}} = + / - \quad (3)$$

The (+) energy value $\Rightarrow E_{d_o} > E_{d_t}$; \therefore t-site has **minimum** energy while the (-) energy value $\Rightarrow E_{d_o} < E_{d_t}$; \therefore o-site has **minimum** energy. This confirms the results of the theoretical formulae by considering the unrelaxed dissolution energy difference of all the bcc-refractory interstitial solid solution from Table 2 - 5 as well as the dissolution energies at the Appdx. A1 - A4. Unfortunately, the relaxed structure was not permitted to conform to the same circumstance under which the theoretical formulae was set up. This is clearly shown for all concentration of the supercells or atleast either the 1st and 2nd supercells for the solid solutions.

Table 2: Dissolution energy difference ($\Delta E_{d_{o-t}}$) between Nitrogen (N) in the o-site and t-site of bcc Molybdenum (Mo) for both unrelaxed (Ur) and relaxed (R) structures

Supercell	$C_N(at.%)$	$\Delta E_{Ur_{o-t}}$ (eV)	$\Delta E_{R_{o-t}}$ (eV)
Mo2N1	33.3	2.0274	-1.4906
Mo16N1	5.88	1.8335	-0.5429
Mo54N1	1.82	2.0287	-0.6960

Starting with the concentration of X_2A cells which may be considered as a supersaturated solution of the interstitial in the bcc refractory metals. Its noticed that there was very high change in the dissolution energy towards the negative as compared to the other concentrations. This depicts stability at the octahedral sites which is in agreement with Table 6 and Figure 3 showing less volumetric strain at the o-site than that of the t-sites.

Table 3: Dissolution energy difference ($\Delta E_{d_{o-t}}$) between Nitrogen (N) in the o-site and t-site of bcc Niobium (Nb) for both unrelaxed (Ur) and relaxed (R) structures

Supercell	$C_N(at.%)$	$\Delta E_{Ur_{o-t}}$ (eV)	$\Delta E_{R_{o-t}}$ (eV)
Nb2N1	33.3	1.3852	-1.6695
Nb16N1	5.88	1.2986	-0.9776
Nb54N1	1.82	1.4313	0.0041

Table 4: Dissolution energy difference ($\Delta E_{d_{o-t}}$) between Oxygen (O) in the o-site and t-site of bcc Molybdenum (Mo) for both unrelaxed (Ur) and relaxed (R) structures

Supercell	$C_O(at.%)$	$\Delta E_{Ur_{o-t}}$ (eV)	$\Delta E_{R_{o-t}}$ (eV)
Mo2O1	33.3	1.7413	-0.5892
Mo16O1	5.88	2.7161	0.3629
Mo54O1	1.82	2.8144	0.0893

Table 5: Dissolution energy difference ($\Delta E_{d_{o-t}}$) between Oxygen (O) in the o-site and t-site of bcc Niobium (Nb) for both unrelaxed (Ur) and relaxed (R) structures

Supercell	$C_O(at.%)$	$\Delta E_{Ur_{o-t}}$ (eV)	$\Delta E_{R_{o-t}}$ (eV)
Nb2O1	33.3	1.4803	-0.1599
Nb16O1	5.88	1.4312	-0.8473
Nb54O1	1.82	1.6656	0.0336

Unlike the unrelaxed structures, there is a change with the preference of the site occupancy when the concentration diminishes. This change of site preference from the o-site to the t-site in the concentration of $X_{16}A$ supercell is ONLY recognised in Mo16O1 (Table 4) which is clearly seen among the other bcc refractory interstitial solid solution. It also shows a clear agreement with the volumetric strain shown in Table 6 even though the Mo16O1 depicts otherwise. This dispute with the dissolution energy difference and the volumetric

strain, may be due to the slight change in shift or distortion as seen in Table 6, which show that the volumetric strain at the o-site and t-site are quite closer as compared to other solid solution.

Table 6: Volumetric strain, $\epsilon_v = (\frac{\Delta V}{V})^*$ for the relaxed (R) cells structure of the interstitial solute, ($A = \{N \text{ or } O\}$) in the Octahedral (o) or Tetrahedral (t) site of the bcc refractory metal ($X = \{Mo \text{ or } Nb\}$)

$C_A (at. \%)$	$Mo_x N1$		$Nb_x N1$		$Mo_x O1$		$Nb_x O1$	
	ϵ_{v_o}	ϵ_{v_t}	ϵ_{v_o}	ϵ_{v_t}	ϵ_{v_o}	ϵ_{v_t}	ϵ_{v_o}	ϵ_{v_t}
33.3	17.0426	28.0075	13.1502	25.7466	18.8283	25.3133	13.5845	30.0358
5.88	3.1029	3.9317	2.7804	4.2476	3.6135	3.9709	2.9754	3.7825
1.82	0.9074	1.0610	1.0028	0.8207	1.0063	1.1168	1.0160	0.6871

* Volume increase of the relaxed $X_x A$ cell with respect to the relaxed X_x cell.

The last supercell shows a complete change to the original site preference proposed by the theoretical formulae (thus, Eqs. [o-site](#) and [t-site](#)) as discussed earlier for all the solid solution except for Mo-N. This complete change again can be linked to the volumetric strain which is in total agreement with the assertion by taking a look at [Figure 3](#) but has a slight contrast as shown in [Table 6](#) with respect to the solid solution Mo-O. This slight contrast between the dissolution energy difference and the volumetric strain, is due to the closeness of the distortion that occur at both sites within the Mo54O1. [Figure 3](#) shows the form of convergence with respect to the distortion and stability when the site preferences are of a concern to all solid solution.

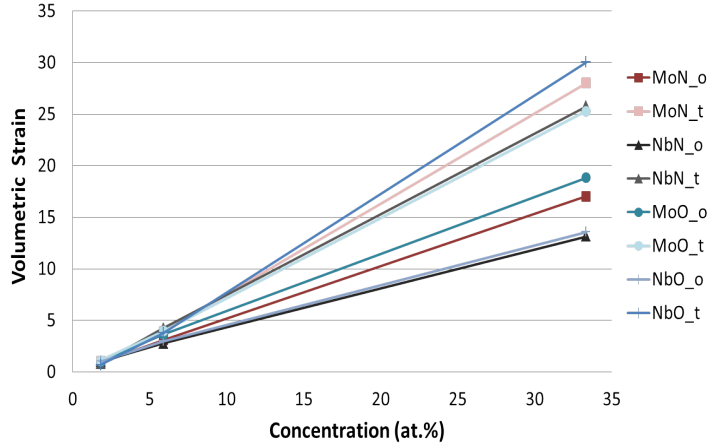


Figure 3: A plot of volumetric strains when an interstitial solute (N or O) is inserted in the Octahedral (o) or Tetrahedral (t) site of a bcc refractory metal (Mo or Nb) at 0 K and relaxed

4. Conclusion

Density Functional Theory calculation was performed to examine the thermodynamic stable site preference on some selected bcc refractory interstitial solid solution. The dissolution mechanism of all the relaxed solid solution structures were predicted to be an exothermic reaction from the supersaturated cell to the low concentration (1.82 at.%) except for Mo-N solid solution. Convergence of volumetric strain was observed moving towards low concentration (1.82 at.%) of the solute with a less measure of global stress (less distortion) at the octahedral (o) site for the solid solutions of Mo-N and Mo-O and at the tetrahedral site for the Nb-N and Nb-O. This certainly shows why the two (2) bcc-refractory metals in groups VB (Nb) and VIB (Mo) of the periodic table exhibit different deformation behaviours giving their difference in site preference stability. We also noted that the demonstration of stability for all the solid solution at less concentration requires further study on the movement of the solute (N or O) across the sites (thus through o-sites, t-sites and o-t-sites) with a very low concentration of the solute or bigger supercell than what was under study in this work.

5. Acknowledgements

Centre for Scientific and Technical Computing, National Institute for Mathematical Sciences hosted by Kwame Nkrumah University of Science and Technology Kumasi, Ghana. The authors would like to thank Prof. Jaime Marian and his group at Department of Materials Science and Engineering and Mechanical and Aerospace Engineering, University of California Los Angeles (UCLA), Los Angeles, USA, for his helpful discussion, insightful advice, access and usage of the computational and storage services associated with the Hoffman2 Shared Cluster provided by UCLA Institute for Digital Research and Education’s Research Technology Group.

6. Appendix

Table A1: Dissolution energy (E_d) of Nitrogen (N) in the Octahedral (o) and Tetrahedral (t) sites of bcc Molybdenum (Mo) for both unrelaxed (Ur) and relaxed (R) structures

Supercell	$C_N(at.%)$	o site		t site	
		$E_{d_{Ur}}$ (eV)	E_{d_R} (eV)	$E_{d_{Ur}}$ (eV)	E_{d_R} (eV)
Mo2N1	33.3	2.9713	-0.6064	0.9439	0.8842
Mo16N1	5.88	5.4796	0.9791	3.6461	1.5220
Mo54N1	1.82	6.0527	0.7795	4.0240	1.4755

Table A2: Dissolution energy (E_d) of Nitrogen (N) in the Octahedral (o) and Tetrahedral (t) sites of bcc Niobium (Nb) for both unrelaxed (Ur) and relaxed (R) structures

Supercell	$C_N(at.%)$	o site		t site	
		$E_{d_{Ur}}$ (eV)	E_{d_R} (eV)	$E_{d_{Ur}}$ (eV)	E_{d_R} (eV)
Nb2N1	33.3	1.0690	-2.1949	-0.3162	-0.5253
Nb16N1	5.88	2.0490	-1.7504	0.7504	-0.7728
Nb54N1	1.82	2.2927	-2.2332	0.8614	-2.2373

Table A3: Dissolution energy (E_d) of Oxygen (O) in the Octahedral (o) and Tetrahedral (t) sites of bcc Molybdenum (Mo) for both unrelaxed (Ur) and relaxed (R) structures

Supercell	$C_N(at.%)$	o site		t site	
		$E_{d_{Ur}}$ (eV)	E_{d_R} (eV)	$E_{d_{Ur}}$ (eV)	E_{d_R} (eV)
Mo2O1	33.3	1.0479	-1.4403	-0.6934	-0.8512
Mo16O1	5.88	4.7204	-0.0226	2.0043	-0.3855
Mo54O1	1.82	5.3028	-0.3552	2.4885	-0.4444

Table A4: Dissolution energy (E_d) of Oxygen (O) in the Octahedral (o) and Tetrahedral (t) sites of bcc Niobium (Nb) for both unrelaxed (Ur) and relaxed (R) structures

Supercell	$C_N(at.%)$	o site		t site	
		$E_{d_{Ur}}$ (eV)	E_{d_R} (eV)	$E_{d_{Ur}}$ (eV)	E_{d_R} (eV)
Nb2O1	33.3	-1.1301	-3.5987	-2.6103	-3.4388
Nb16O1	5.88	0.3354	-3.6867	-1.0958	-2.8394
Nb54O1	1.82	0.6030	-4.0744	-1.0627	-4.1080

(+) pos energy value - endothermic process of dissolution.

(-) neg energy value - exothermic process of dissolution

References

References

- [1] J. R. Davis, Alloying: understanding the basics, ASM international, 2001.
- [2] M. Baucchio, ASM metals reference book "Refractory metals", ASM international, 1993.
- [3] F. Habashi, Historical introduction to refractory metals, Mineral Processing and Extractive Metallurgy Review 22 (1) (2001) 25–53.
- [4] J. Kepler, C. G. Hardie, B. J. Mason, L. L. Whyte, The Six-cornered Snowflake Lat. & Eng, Clarendon Press, 1966.
- [5] T. Hales, M. Adams, G. Bauer, T. D. Dang, J. Harrison, H. Le Truong, C. Kaliszyk, V. Magron, S. McLaughlin, T. T. Nguyen, et al., A formal proof of the kepler conjecture, in: Forum of Mathematics, Pi, Vol. 5, Cambridge University Press, 2017. [doi:10.1017/fmp.2017.1](https://doi.org/10.1017/fmp.2017.1).
- [6] J. Christian, Some surprising features of the plastic deformation of body-centered cubic metals and alloys, Metallurgical Transactions A 14 (7) (1983) 1237–1256. [doi:10.1007/BF02664806](https://doi.org/10.1007/BF02664806).
- [7] D. Caillard, J.-L. Martin, Thermally activated mechanisms in crystal plasticity, Vol. 8, Elsevier, 2003.
- [8] A. S. Argon, Strengthening mechanisms in crystal plasticity, Vol. 4, Oxford University Press, 2008.
- [9] A. Seeger, The flow stress of high-purity refractory body-centred cubic metals and its modification by atomic defects, Le Journal de Physique IV 5 (C7) (1995) C745–C765. [doi:10.1051/jp4:1995704](https://doi.org/10.1051/jp4:1995704).
- [10] W. Pichl, Slip geometry and plastic anisotropy of body-centered cubic metals, physica status solidi (a) 189 (1) (2002) 5–25. [doi:10.1002/1521-396X\(200201\)189:1<5::AID-PSSA5>3.0.CO;2-D](https://doi.org/10.1002/1521-396X(200201)189:1<5::AID-PSSA5>3.0.CO;2-D).

- [11] A. Stukowski, D. Cereceda, T. D. Swinburne, J. Marian, Thermally-activated non-schmid glide of screw dislocations in w using atomistically-informed kinetic monte carlo simulations, *International Journal of Plasticity* 65 (2015) 108–130. doi:10.1016/j.ijplas.2014.08.015.
- [12] D. Cereceda, M. Diehl, F. Roters, D. Raabe, J. M. Perlado, J. Marian, Unraveling the temperature dependence of the yield strength in single-crystal tungsten using atomistically-informed crystal plasticity calculations, *International Journal of Plasticity* 78 (2016) 242–265. doi:10.1016/j.ijplas.2015.09.002.
- [13] J. Chaussidon, M. Fivel, D. Rodney, The glide of screw dislocations in bcc fe: Atomistic static and dynamic simulations, *Acta materialia* 54 (13) (2006) 3407–3416. doi:10.1016/j.actamat.2006.03.044.
- [14] S. Brinckmann, J.-Y. Kim, J. R. Greer, Fundamental differences in mechanical behavior between two types of crystals at the nanoscale, *Physical review letters* 100 (15) (2008) 155502. doi:10.1103/PhysRevLett.100.155502.
- [15] P. Penning, Mathematics of the portevin-le chatelier effect, *Acta Metallurgica* 20 (10) (1972) 1169–1175. doi:10.1016/0001-6160(72)90165-4.
- [16] D. R. Trinkle, C. Woodward, The chemistry of deformation: How solutes soften pure metals, *Science* 310 (5754) (2005) 1665–1667. doi:10.1126/science.1118616.
- [17] L. Romaner, C. Ambrosch-Draxl, R. Pippan, Effect of rhenium on the dislocation core structure in tungsten, *Physical review letters* 104 (19) (2010) 195503. doi:10.1103/PhysRevLett.104.195503.
- [18] H. Li, S. Wurster, C. Motz, L. Romaner, C. Ambrosch-Draxl, R. Pippan, Dislocation-core symmetry and slip planes in tungsten alloys: Ab initio calculations and microcantilever bending experiments, *Acta Materialia* 60 (2) (2012) 748–758. doi:10.1016/j.actamat.2011.10.031.

- [19] G. D. Samolyuk, Y. Osetsky, R. Stoller, The influence of transition metal solutes on the dislocation core structure and values of the peierls stress and barrier in tungsten, *Journal of Physics: Condensed Matter* 25 (2) (2012) 025403. doi:[10.1088/0953-8984/25/2/025403](https://doi.org/10.1088/0953-8984/25/2/025403).
- [20] M. S. Duesbery, V. Vitek, Plastic anisotropy in bcc transition metals, *Acta Materialia* 46 (5) (1998) 1481–1492. doi:[10.1016/S1359-6454\(97\)00367-4](https://doi.org/10.1016/S1359-6454(97)00367-4).
- [21] C. R. Weinberger, B. L. Boyce, C. C. Battaile, Slip planes in bcc transition metals, *International Materials Reviews* 58 (5) (2013) 296–314. doi:[10.1179/1743280412Y.0000000015](https://doi.org/10.1179/1743280412Y.0000000015).
- [22] C. R. Weinberger, G. J. Tucker, S. M. Foiles, Peierls potential of screw dislocations in bcc transition metals: Predictions from density functional theory, *Physical Review B* 87 (5) (2013) 054114. doi:[10.1103/PhysRevB.87.054114](https://doi.org/10.1103/PhysRevB.87.054114).
- [23] H. Lim, C. R. Weinberger, C. C. Battaile, T. E. Buchheit, Application of generalized non-schmid yield law to low-temperature plasticity in bcc transition metals, *Modelling and Simulation in Materials Science and Engineering* 21 (4) (2013) 045015. doi:[10.1088/0965-0393/21/4/045015](https://doi.org/10.1088/0965-0393/21/4/045015).
- [24] H. Lim, C. C. Battaile, C. R. Weinberger, Simulating dislocation plasticity in bcc metals by integrating fundamental concepts with macroscale models, *Integrated Computational Materials Engineering (ICME) for Metals: Concepts and Case Studies* (2018) 71–105doi:[10.1002/9781119018377.ch4](https://doi.org/10.1002/9781119018377.ch4).
- [25] C. Woodward, S. I. Rao, Ab-initio simulation of isolated screw dislocations in bcc mo and ta, *Philosophical Magazine A* 81 (5) (2001) 1305–1316. doi:[10.1080/01418610108214442](https://doi.org/10.1080/01418610108214442).
- [26] L. Dezerald, L. Proville, L. Ventelon, F. Willaime, D. Rodney, First-principles prediction of kink-pair activation enthalpy on screw dislocations

- in bcc transition metals: V, nb, ta, mo, w, and fe, *Physical Review B* 91 (9) (2015) 094105. doi:10.1103/PhysRevB.91.094105.
- [27] L. Dezerald, D. Rodney, E. Clouet, L. Ventelon, F. Willaime, Plastic anisotropy and dislocation trajectory in bcc metals, *Nature communications* 7 (2016) 11695. doi:10.1038/ncomms11695.
- [28] D. Rodney, L. Ventelon, E. Clouet, L. Pizzagalli, F. Willaime, Ab initio modeling of dislocation core properties in metals and semiconductors, *Acta Materialia* 124 (2017) 633–659. doi:10.1016/j.actamat.2016.09.049.
- [29] M. Hansen, K. Anderko, H. Salzberg, Constitution of binary alloys, *Journal of the Electrochemical Society* 105 (12) (1958) 260C–261C. doi:10.1149/1.2428700.
- [30] J. B. Austin, *Edgar collins bain*, *Biographical Memoirs* 49 (1978) 25.
URL www.nasonline.org/publications/biographical-memoirs/memoir-pdfs/bain-edgar-c.pdf
- [31] H. Martin, P. Amoako-Yirenkyi, A. Pohjonen, N. K. Frempong, J. Komi, M. Somani, Statistical modeling for prediction of cct diagrams of steels involving interaction of alloying elements, *Metallurgical and Materials Transactions B* (2020) 1–13doi:10.1007/s11663-020-01991-w.
- [32] H. Martin, A statistical and quantum mechanical model of combined alloying elements for phase transformation, *Theses*, Kwame Nkrumah University of Science and Technology, Kumasi, Ghana (2019).
- [33] M. Henry, N. Oswald, B. C. D. Andrew, Improve the ductility of locally manufactured steel rods by tempering, in: 27th Biennial Conference Proceeding, *Journal of the Ghana Science Association*, 2011.
- [34] N. Medvedeva, Y. N. Gornostyrev, A. Freeman, Solid solution softening and hardening in the group-v and group-vi bcc transition metals alloys: First principles calculations and atomistic modeling, *Physical Review B* 76 (21) (2007) 212104. doi:10.1103/PhysRevB.76.212104.

- [35] Y. Zhao, G. Lu, Qm/mm study of dislocation-hydrogen/helium interactions in α -fe, *Modelling and Simulation in Materials Science and Engineering* 19 (6) (2011) 065004. doi:[10.1088/0965-0393/19/6/065004](https://doi.org/10.1088/0965-0393/19/6/065004).
- [36] M. Itakura, H. Kaburaki, M. Yamaguchi, T. Okita, The effect of hydrogen atoms on the screw dislocation mobility in bcc iron: a first-principles study, *Acta Materialia* 61 (18) (2013) 6857–6867. doi:[10.1016/j.actamat.2013.07.064](https://doi.org/10.1016/j.actamat.2013.07.064).
- [37] L. Romaner, V. Razumovskiy, R. Pippan, Core polarity of screw dislocations in fe-co alloys, *Philosophical Magazine Letters* 94 (6) (2014) 334–341. doi:[10.1080/09500839.2014.904055](https://doi.org/10.1080/09500839.2014.904055).
- [38] L. Ventelon, B. Lüthi, E. Clouet, L. Proville, B. Legrand, D. Rodney, F. Willaime, Dislocation core reconstruction induced by carbon segregation in bcc iron, *Physical Review B* 91 (22) (2015) 220102. doi:[10.1103/PhysRevB.91.220102](https://doi.org/10.1103/PhysRevB.91.220102).
- [39] Y.-J. Hu, M. R. Fellingner, B. G. Bulter, Y. Wang, K. A. Darling, L. J. Kecskes, D. R. Trinkle, Z.-K. Liu, Solute-induced solid-solution softening and hardening in bcc tungsten, *Acta Materialia* 141 (2017) 304–316. doi:[10.1016/j.actamat.2017.09.019](https://doi.org/10.1016/j.actamat.2017.09.019).
- [40] Y. Zhao, J. Marian, Direct prediction of the solute softening-to-hardening transition in w-re alloys using stochastic simulations of screw dislocation motion, *Modelling and Simulation in Materials Science and Engineering* 26 (4) (2018) 045002. doi:[10.1088/1361-651X/aaecf](https://doi.org/10.1088/1361-651X/aaecf).
- [41] B. Lüthi, L. Ventelon, C. Elsässer, D. Rodney, F. Willaime, First principles investigation of carbon-screw dislocation interactions in body-centered cubic metals, *Modelling and Simulation in Materials Science and Engineering* 25 (8) (2017) 084001. doi:[10.1088/1361-651X/aa88eb](https://doi.org/10.1088/1361-651X/aa88eb).
- [42] J. Svoboda, F. Fischer, Anisotropy of interstitial diffusion in bcc-crystals due to stress-induced unequal occupancies of different types of sites, *Inter-*

- national Journal of Solids and Structures [doi:10.1016/j.ijsolstr.2018.05.023](https://doi.org/10.1016/j.ijsolstr.2018.05.023).
- [43] Y. Zhao, L. Dezerald, J. Marian, Electronic structure calculations of oxygen atom transport energetics in the presence of screw dislocations in tungsten, *Metals* 9 (2) (2019) 252. [doi:10.3390/met9020252](https://doi.org/10.3390/met9020252).
- [44] B. Lüthi, L. Ventelon, D. Rodney, F. Willaime, Attractive interaction between interstitial solutes and screw dislocations in bcc iron from first principles, *Computational Materials Science* 148 (2018) 21–26. [doi:10.1016/j.commatsci.2018.02.016](https://doi.org/10.1016/j.commatsci.2018.02.016).
- [45] Y. Wang, X. Wang, Q. Li, B. Xu, W. Liu, Atomistic simulations of carbon effect on kink-pair energetics of bcc iron screw dislocations, *Journal of Materials Science* 54 (15) (2019) 10728–10736. [doi:10.1007/s10853-019-03564-y](https://doi.org/10.1007/s10853-019-03564-y).
- [46] J. R. Stephens, [Effects of interstitial impurities on the low-temperature tensile properties of tungsten](#), Tech. rep., National Aeronautics and Space Administration Cleveland OH Lewis Research Center (1964).
URL <https://apps.dtic.mil/docs/citations/ADA396979>
- [47] M. Ulitchny, R. Gibala, The effects of interstitial solute additions on the mechanical properties of niobium and tantalum single crystals, *Journal of the Less Common Metals* 33 (1) (1973) 105–116. [doi:10.1016/0022-5088\(73\)90061-1](https://doi.org/10.1016/0022-5088(73)90061-1).
- [48] X. Jiang, M. Wang, K. Schmidt, E. Dunlop, J. Haupt, W. Gissler, Elastic constants and hardness of ion-beam-sputtered tin x films measured by brillouin scattering and depth-sensing indentation, *Journal of applied physics* 69 (5) (1991) 3053–3057. [doi:10.1063/1.348963](https://doi.org/10.1063/1.348963).
- [49] S.-H. Jhi, S. G. Louie, M. L. Cohen, J. Ihm, Vacancy hardening and softening in transition metal carbides and nitrides, *Physical Review Letters* 86 (15) (2001) 3348. [doi:10.1103/PhysRevLett.86.3348](https://doi.org/10.1103/PhysRevLett.86.3348).

- [50] X.-J. Chen, V. V. Struzhkin, Z. Wu, M. Somayazulu, J. Qian, S. Kung, A. N. Christensen, Y. Zhao, R. E. Cohen, H.-k. Mao, et al., Hard superconducting nitrides, *Proceedings of the National Academy of Sciences* 102 (9) (2005) 3198–3201. doi:[10.1073/pnas.0500174102](https://doi.org/10.1073/pnas.0500174102).
- [51] Z. Wu, X.-J. Chen, V. V. Struzhkin, R. E. Cohen, Trends in elasticity and electronic structure of transition-metal nitrides and carbides from first principles, *Physical Review B* 71 (21) (2005) 214103. doi:[10.1103/PhysRevB.71.214103](https://doi.org/10.1103/PhysRevB.71.214103).
- [52] R. Hickman, T. McKechnie, Advanced materials and processes for boost phase nozzles, in: 40th AIAA/ASME/SAE/ASEE Joint Propulsion Conference and Exhibit, 2004, p. 3385. doi:[10.2514/6.2004-3385](https://doi.org/10.2514/6.2004-3385).
- [53] P. Thakre, V. Yang, Chemical erosion of refractory-metal nozzle inserts in solid-propellant rocket motors, *Journal of Propulsion and Power* 25 (1) (2009) 40–50. doi:[10.2514/1.37922](https://doi.org/10.2514/1.37922).
- [54] J.-Y. Yan, A. Ruban, Configurational thermodynamics of c in body-centered cubic/tetragonal fe: A combined computational study, *Computational Materials Science* 147 (2018) 293–303. doi:[10.1016/j.commatsci.2018.02.024](https://doi.org/10.1016/j.commatsci.2018.02.024).
- [55] P. Hohenberg, W. Kohn, *Inhomogeneous electron gas*, *Physical review* 136 (3B) (1964) B864. doi:[10.1103/PhysRev.136.B864](https://doi.org/10.1103/PhysRev.136.B864).
URL <https://doi.org/10.1103/PhysRev.136.B864>
- [56] W. Kohn, L. J. Sham, *Self-consistent equations including exchange and correlation effects*, *Physical review* 140 (4A) (1965) A1133.
URL <https://doi.org/10.1103/PhysRev.140.A1133>
- [57] G. Kresse, J. Furhmüller, Software vasp, vienna (1999); g. kresse, j. hafner, *Phys. Rev. B* 47 (R558).
- [58] G. Kresse, J. Furthmüller, *Efficient iterative schemes for ab initio total-energy calculations using a plane-wave basis set*, *Physical review B* 54 (16)

- (1996) 11169.
URL <https://doi.org/10.1103/PhysRevB.54.11169>
- [59] G. Kresse, J. Furthmüller, Efficiency of ab-initio total energy calculations for metals and semiconductors using a plane-wave basis set, *Computational materials science* 6 (1) (1996) 15–50. doi:10.1016/0927-0256(96)00008-0.
- [60] P. E. Blöchl, [Projector augmented-wave method](#), *Physical review B* 50 (24) (1994) 17953.
URL <https://doi.org/10.1103/PhysRevB.50.17953>
- [61] G. Kresse, D. Joubert, [From ultrasoft pseudopotentials to the projector augmented-wave method](#), *Physical Review B* 59 (3) (1999) 1758.
URL <https://doi.org/10.1103/PhysRevB.59.1758>
- [62] A. Dewaele, M. Torrent, P. Loubeyre, M. Mezouar, Compression curves of transition metals in the mbar range: Experiments and projector augmented-wave calculations, *Physical Review B* 78 (10) (2008) 104102.
- [63] B. J. Min, Study of the electronic and the structural properties of small molybdenum clusters via projector augmented wave pseudopotential calculations, *Journal of the Korean Physical Society* 66 (2) (2015) 209–213.
- [64] L. Liang, [Ab initio simulation of extended defects of \$\alpha\$ -Ti in presence of interstitial atoms H & O](#), Theses, Université Paris-Saclay (2016).
URL <https://pastel.archives-ouvertes.fr/tel-01355132>
- [65] J. P. Perdew, K. Burke, M. Ernzerhof, [Generalized gradient approximation made simple](#), *Physical review letters* 77 (18) (1996) 3865. doi:10.1103/PhysRevLett.77.3865.
URL <https://doi.org/10.1103/PhysRevLett.77.3865>
- [66] J. P. Perdew, M. Ernzerhof, A. Zupan, K. Burke, Nonlocality of the density functional for exchange and correlation: Physical origins and chemical

- consequences, *The Journal of chemical physics* 108 (4) (1998) 1522–1531. doi:10.1063/1.475524.
- [67] A. Zupan, K. Burke, M. Ernzerhof, J. P. Perdew, Distributions and averages of electron density parameters: Explaining the effects of gradient corrections, *The Journal of chemical physics* 106 (24) (1997) 10184–10193. doi:10.1063/1.474101.
- [68] A. Baldereschi, Mean-value point in the brillouin zone, *Physical Review B* 7 (12) (1973) 5212.
- [69] H. J. Monkhorst, J. D. Pack, [Special points for brillouin-zone integrations](#), *Physical review B* 13 (12) (1976) 5188. doi:10.1103/PhysRevB.13.5188. URL <https://doi.org/10.1103/PhysRevB.13.5188>
- [70] M. Methfessel, A. Paxton, [High-precision sampling for brillouin-zone integration in metals](#), *Physical Review B* 40 (6) (1989) 3616. URL <https://doi.org/10.1103/PhysRevB.40.3616>
- [71] D. D. Johnson, Modified broyden’s method for accelerating convergence in self-consistent calculations, *Physical Review B* 38 (18) (1988) 12807.
- [72] W. P. Davey, Precision measurements of the lattice constants of twelve common metals, *Physical Review* 25 (6) (1925) 753.
- [73] C. Kittel, P. McEuen, P. McEuen, *Introduction to solid state physics*, Vol. 8, Wiley New York, 1996.
- [74] K. Hermann, *Crystallography and Surface Structure: An Introduction for Surface Scientists and Nanoscientists*, 2nd Edition, Wiley-VCH Verlag GmbH & Co. KGaA, 2017.
- [75] E. I. Isaev, S. I. Simak, I. Abrikosov, R. Ahuja, Y. K. Vekilov, M. Katsnelson, A. Lichtenstein, B. Johansson, Phonon related properties of transition metals, their carbides, and nitrides: A first-principles study, *Journal of applied physics* 101 (12) (2007) 123519. doi:10.1063/1.2747230.

- [76] D. E. Gray, et al., American Institute of Physics handbook: Section editors: Bruce H. Billings [and others] Coordinating editor: Dwight E. Gray, McGraw-Hill Companies, 1972.
- [77] M. Delheusy, X-ray investigation of nb/o interfaces, Theses, Universite Paris-Sud XI (2008). [doi:10.18419/opus-6994](https://doi.org/10.18419/opus-6994).
- [78] T. Amriou, B. Bouhafs, H. Aourag, B. Khelifa, S. Bresson, C. Mathieu, Fp-lapw investigations of electronic structure and bonding mechanism of nbc and nbn compounds, Physica B: Condensed Matter 325 (2003) 46–56. [doi:10.1016/S0921-4526\(02\)01429-1](https://doi.org/10.1016/S0921-4526(02)01429-1).
- [79] P. Haas, F. Tran, P. Blaha, Calculation of the lattice constant of solids with semilocal functionals, Physical Review B 79 (8) (2009) 085104.
- [80] D. Connétable, First-principles study of transition metal carbides, Materials Research Express 3 (12) (2016) 126502. [doi:10.1088/2053-1591/3/12/126502](https://doi.org/10.1088/2053-1591/3/12/126502).
- [81] T. Shimanouchi, Tables of molecular vibrational frequencies part 5, Journal of Physical and Chemical Reference Data 1 (1) (1972) 189–216.
- [82] J. Gutow, A. Herráez, Nitrogen gas (n2), Tech. rep., University of Wisconsin Oshkosh (UWOSH) (2009).
URL http://www.uwosh.edu/faculty_staff/gutow/Chem_371_S09/OASI%20Web%20Pages/N2%20Calculations/N2%20Calculations/N2%20Calculations.html
- [83] A. Weber, E. A. McGinnis, The raman spectrum of gaseous oxygen, Journal of Molecular Spectroscopy 4 (1-6) (1960) 195–200. [doi:10.1016/0022-2852\(60\)90081-3](https://doi.org/10.1016/0022-2852(60)90081-3).
- [84] W. McGrath, A. R. J. P. Ubbelohde, The influence of molecular flexibility on the transfer of vibrational energy in hydrocarbons, Proceedings of the Royal Society of London. Series A. Mathematical and Physical Sciences 227 (1168) (1954) 1–9. [doi:10.1098/rspa.1954.0275](https://doi.org/10.1098/rspa.1954.0275).